Limnol. Oceanogr., 43(5), 1998, 847–858

Light scattering and chlorophyll concentration in case 1 waters: A reexamination

Hubert Loisel and André Morel
Laboratoire de Physique et Chimie Marines, Université Pierre et Marie Curie and CNRS, BP8, F 06238 Villefranche-sur mer CEDEX, France

Abstract

An analysis is presented based on a large dataset (N = 2,787) made up of recent measurements of the beam attenuation coefficient at 660 nm and of the chlorophyll concentration by using the SeaTech transmissometer and the high-pressure liquid chromatography technique, respectively. This analysis, restricted to case 1 waters, aims at reassessing a previous nonlinear relationship established between the particle scattering coefficient, b_p (very close to the particle attenuation coefficient, c_p), and the chlorophyll concentration, [Chl]. As a first result, nonlinearity is fully confirmed over the whole range of oceanic chlorophyll concentration (about 3 orders of magnitude). Despite more accurate measurements, the scatter in this relationship remains large and is actually comparable to that observed within the old dataset. Rather than establishing a single relationship between c_p (or b_p) and [Chl] for the entire upper water column, the deep layer and the near-surface layer (important for remote-sensing application) have been studied separately. This separation has led to two distinct expressions. A more appropriate parameterization is thus proposed when dealing specifically with, and modeling, the near-surface layer. As a consequence, a modified criterion is also suggested with a view to identifying turbid case 2 waters.

Understanding or predicting the propagation of radiant energy within a water body requires that the boundary conditions (at the interface and bottom) and the inherent optical properties (IOP) within the medium are both known or prescribed. Strictly speaking, these properties (IOP) within the medium are both known or prescribed. Strictly speaking, these properties comprise the absorption coefficient, a, and the volume scattering function $\beta(\theta)$; the scattering coefficient, b, derives from $\beta(\theta)$ by integrating over the whole space, and the attenuation coefficient, c, represents the sum of a and b. These last three coefficients are expressed as m^{-1}. The IOP result from the presence in a water body of colored dissolved organic substances and of scattering as well as absorbing particulate matter.

In the open ocean, far from notable terrigenous influence, these optically active materials are locally and permanently formed through various processes along the trophic chain. These oceanic waters are commonly referred to as case 1 waters (Morel and Prieur 1977). For historical and practical reasons, the index usually adopted to specify the bio-optical state (Smith and Baker 1978) of a water body is its chlorophyll a concentration, hereafter simply denoted as [Chl] (expressed in mg m^{-3}). This adoption acknowledges that in many oceanic environments, and in case 1 waters by definition, phytoplankton with their associated and derivative products play a major role in determining the IOP. As a result, optical modeling of case 1 waters requires that relationships between the IOP and [Chl] are available for the whole range of possible variations in [Chl]. In the upper layers of these waters, [Chl] may vary from nearly zero (i.e. ~0.02 mg m^{-3}) up to 20 mg m^{-3} or even more from oligotrophic to eutrophic situations. The present study deals with recent field measurements specifically performed in case 1 waters and aims at reexamining the relationships between the scattering coefficient and [Chl]. The scattering coefficient, or more accurately its varying part, denoted b_p (the constant part originates from the scattering of water molecules), results from the presence of all kinds of suspended matter, such as autotrophic, small heterotrophic living organisms, as well as from detritus of various sizes. Among these particles, only phytoplanktonic cells bear chlorophyll (some of their predators may also). Importantly, [Chl] is a descriptor of only one fraction of the particle population; therefore, trying to relate b_p to [Chl] admittedly induces some inevitable uncertainties.

Based on previous field determinations in the tropical Atlantic and Pacific Oceans and on their statistical analyses, a first empirical relationship was presented (Morel 1980) and then slightly modified after additional data were included (Gordon and Morel 1983). This relationship, for case 1 waters only (with 659 pairs of data), was established for the particle scattering coefficient, b_p, determined at the wavelength 550 nm, and for [Chl] spanning about three orders of magnitude. The relationship was

Acknowledgments

OMEX data were made available with the originators' permission from the EU-MAST OMEX 1 Programme by the British Oceanographic Data center (BODC). The HPLC chlorophyll measurements for this project were undertaken by R. Barlow and R. F. C. Mantoura at the Plymouth Laboratory. They are gratefully acknowledged for having made their data available to us. The transmissometer data for the same cruise were calibrated and quality controlled by the BODC. We thank R. Lowry for his help in the control of, and access to, these data. The BOFS data, published on a CD-ROM, were also produced under the BODC, and are duly appreciated here. The HPLC data for the EUMELI and OLIPAC (French JGOFS) cruises and those (unpubl.) for the MINOS campaign were performed by H. Claustre with the collaboration of J. C. Marty, C. Cailliau, and F. Vidussi. We thank them for these data. We also thank H. Claustre for helpful suggestions and discussions on a first draft of this paper: Substantial help with fieldwork and maintenance-calibration of the transmissometers used during the French cruises were provided by D. Tailliez, who is gratefully thanked. We acknowledge and thank our colleagues who worked at the two U.S. JGOFS–WOCE time-series and during the EqPac cruises or were involved in the related databanks—these colleagues rendered this study feasible through their continuous effort. This work is a contribution to the French JGOFS Programme "Prosope."

Table 1. Relevant information concerning the data used in this study (N_{sat}, subset of data "seen" by a satellite-borne sensor; N_{hl}, subset of data within homogeneous layers; N_{all}, all data).

	Cruise	N_{sat}	Chl range (mg m^{-3})	N_{hl}	Chl range (mg m^{-3})	N_{all}	Chl range (mg m^{-3})
Apr–Jul 1989–1990	BOFS	77	0.511–3.770	149	0.275–3.770	280	0.0027–3.77
Jan–Jun–Sep 1995	OMEX	32	0.202–1.490	91	0.113–1.490	204	0.005–1.49
Oct 1991	EUMELI 3	26	0.070–0.350	33	0.070–0.350	145	0.026–1.00
Jun 1992	EUMELI 4	45	0.037–2.010	65	0.043–4.530	158	0.01–4.53
Feb–Mar 1992	EqPac	32	0.062–0.251	96	0.062–0.276	473	0.012–0.332
Nov 1994	OLIPAC	63	0.030–0.202	113	0.030–0.230	331	0.02–0.39
Jun 1996	MINOS	103	0.032–0.138	148	0.032–0.217	513	0.022–1.51
1991–1995	HOTS	25	0.0550–0.113	81	0.055–0.138	308	0.003–0.375
1989–1993	BATS	32	0.018–0.330	74	0.018–0.330	375	0.002–0.675
1989–1996	Total	435	0.018–3.770	850	0.018–4.530	2,787	0.002–4.53

$$b_p(550) = A[\text{Chl}]^{0.62}, \quad (1)$$

where [Chl] represents the concentration in both Chl *a* and pheophytin *a*, and where the coefficient *A*, which is on average 0.30 within the upper oceanic layer, may vary between 0.12 and 0.45 to account for the lowest and highest particle scattering coefficients found at various depths in waters satisfying the criterion for belonging to case 1 waters (*see* fig. 5a in Gordon and Morel 1983). The first important result of this previous study was the finding of the nonlinear character of the *b*–[Chl] dependency, as expressed by the exponent 0.62. The second result was the lack of tightness in this relationship, as expressed by the wide possible variations in *A*. As far as we know, the above expression, commonly employed in bio-optical studies and models, has never been reassessed since, except by Voss (1992), who examined a set of 50 data and provided another (albeit similar) relationship between c_p and [Chl], which will be examined later.

The data on which Eq. 1 rests were obtained in the 1970s and were not derived from simultaneous determinations. Indeed, the scattering coefficient was measured with a profiling calibrated instrument, whereas samples for chlorophyll determinations were taken separately during classical hydrocasts using Niskin bottles. The chlorophyll (and pheophytin) determinations were then carried out either spectrophotometrically according to the trichromatic method (Jeffrey and Humphrey 1975) or by the fluorimetric technique (Holm-Hansen et al. 1965), which have potential errors when Chl *b* is present (Gibbs 1979); in particular, such errors may lead to an artifactual overestimate of pheopigment concentration.

The varying chlorophyll-specific scattering coefficient of phytoplanktonic species (Morel 1987), as well as the variable contribution of heterotrophs and detritus, provides some explanations of the nonlinearity and variability in Eq. 1 (Morel and Ahn 1991). It is plausible, however, that the scatter in the original figure of Gordon and Morel originates, at least in part, from the nonsimultaneity of the measurements of the two parameters. Some inconsistencies in the [Chl] determinations owing to changes in methods and experimenters are also likely. Reducing the persisting uncertainties in Eq. 1 and improving the predictive skill of this expression is desirable, if feasible, as weaknesses when modeling case 1 waters originate to a large extent from the approximate character of this relationship.

The vertical profile of the attenuation coefficient, *c*, at a wavelength of 660 nm, is now routinely measured in a continuous way by using transmissometers, such as the SeaTech transmissometer (Bartz et al. 1978). At this wavelength, and once the attenuation by pure seawater has been subtracted, the particle attenuation coefficient is chiefly (~97%; *see below*) due to particle scattering. The transmissometer can be attached to a CTD sensor equipped with a rosette sampling device, so that perfect coincidences between optical measurement and sampling are now achievable. More accurate determinations of the Chl *a* (and divinyl-Chl *a*) are presently possible (and actually recommended; cf. JGOFS protocols) by using high-pressure liquid chromatography (HPLC). Therefore, the validity of the above relationship can be reexamined more accurately than was possible 20 years ago.

Data and methods

Several datasets, consistent in terms of methodologies (SeaTech transmissometer and HPLC), have been considered for the present reexamination. Relevant information is summarized in Table 1. The locations where these measurements have been carried out, all in case 1 waters, are displayed in Fig. 1. They include two permanent time-series stations, at the BATS and HOTS sites (near Bermuda and Hawaii, respectively; Karl and Michaels 1996), as well as stations occupied during specific cruises in the Mediterranean Sea and in the tropical Pacific and Atlantic Oceans. The EUMELI cruises (Fig. 1) were planned to study eutrophic, mesotrophic, and oligotrophic regimes (hence the acronym), and the locations of the three stations were selected accordingly (Morel 1996). The eutrophic site (E site, 140 km of the coast) is located close to the permanent Mauritanian upwelling, the oligotrophic site (O site) in the North Atlantic gyre (1,400 km offshore), and the mesotrophic site (M site) in an intermediate position (400 km offshore).

The [Chl] range encompassed by these data extends from <0.01 mg m^{-3} to ~4.5 mg m^{-3}; these values were observed between the surface and a depth of ~200 m (*see* Table 1). The [Chl] quantity is actually the sum of the concentrations in Chl *a* and divinyl-Chl *a* (when present), whereas pheopigment concentrations, generally found to be insignificant, are not included in [Chl]. The highest [Chl] values were

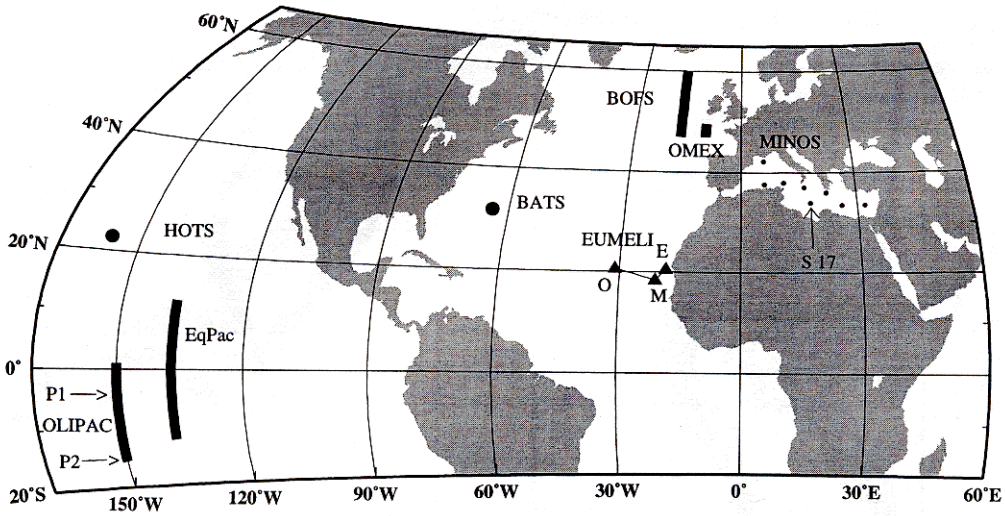

Fig. 1. Locations and transects where the data used in the present study were obtained (*see* also Table 1). The Hawaiian Ocean Time-Series (HOTS) the Bermuda Atlantic Time-Series (BATS) (Karl and Michaels 1996), the British Ocean Flux Study (BOFS; Lowry et al. 1994; and OMEX), the JGOFS–France EUMELI cruises (Morel 1996), the U.S. JGOFS EqPac cruises (Murray et al. 1995), the JGOFS–France OLIPAC cruise (Coste unpubl.), and the recent MINOS French cruise (Raimbault unpubl.) are included. The eutrophic, mesotrophic, and oligotrophic sites visited during the EUMELI program are identified on the map by the letters E, M, and O; P1 and P2 represent 6-d stations (at 5°S, 16°S, and 150°W), and S-17 represents a 3-d station occupied during the MINOS cruise.

systematically observed at the E site occupied during the EUMELI cruise No. 4 (Morel 1996). High values were also commonly observed at the M site and during the spring bloom in the North Atlantic, at the BOFS and OMEX stations (Lowry et al. 1994). The lowest values (i.e. <0.1 mg m^{-3}) belong to two categories—they were observed either in deep samples in mesotrophic, eutrophic, and bloom situations, or in the upper layers, when oligotrophic conditions prevailed. Such conditions were permanently encountered in the oligotrophic EUMELI site, the HOT site, in the Eastern Mediterranean Sea in June, in the OLIPAC and EqPac stations outside of the equatorial divergence (see Fig. 2), and in the BATS site (most of the time, except in early spring). Mesotrophic conditions, with intermediate [Chl] values, between 0.1 and 1 mg m^{-3} in the upper layer, are also included in the datasets. They were observed at the mesotrophic EUMELI site, near the equator in the Pacific Ocean (EqPac, OLIPAC), anywhere in the eastern North Atlantic, near Bermuda in spring, and in some locations in the western Mediterranean Sea. In total, for all locations and all depths, 2,787 pairs of c_p–[Chl] data have been gathered (Table 1).

A general feature, typical of oligotrophic situations, is the existence of a deep chlorophyll maximum (DCM) that develops in the stratified portion of the water column below the nutrient-depleted mixed layer (*see* examples in Fig. 2). The [Chl] values in this DCM, generally in the range 0.25–0.50 mg m^{-3}, are similar to those encountered within the near-surface layer in mesotrophic conditions. Because the [Chl] increase in the DCM generally reflects an increase in the chlorophyll content per cell (Kiefer et al. 1976; Cullen 1982; Pak et al. 1988; Kitchen and Zaneveld 1990), rather than an increase in the algal cells numbers (and thus in scattering particles), it seems judicious to consider separately the optical properties in such deep layers and those in the upper mixed layer. In addition, for remote-sensing applications, only the upper layers are involved, so that their optical properties, insofar they may differ from those in the whole euphotic layer, have to be specifically studied. The thickness (Z_{90}) of such near-surface layers "seen" by a satellite-borne sensor is equal to one penetration depth (Gordon and McCluney 1975), i.e. a depth approximately equal to one-fourth of the euphotic depth (as adopted here). For the present dataset, the euphotic depth was either determined at sea or, in absence of measurement, computed by using the vertical chlorophyll profiles and the algorithms developed in Morel (1988) and Morel and Berthon (1989).

Therefore, in view of performing this separate analysis, a subset has been formed that includes only those data (N_{sat} = 435; *see* Table 2) that pertain to the Z_{90} layer as defined above. Visual inspection of all [Chl] and c_p profiles, together with the density profiles, has shown, not unexpectedly, that in most situations the [Chl] is essentially constant within the mixed layer and thus extends deeper than the satellite-sensed layer. Therefore, another subset has been formed that includes all the paired data belonging to these homogeneous layers with quasi-uniform chlorophyll profiles. This subset, which contains more couples (N_{hl} = 850; Table 2), obviously contains the 435 couples already selected for the previous subset. A third subset is composed of data pertaining to the deep layer, below the homogeneous layer (N_{dl} = 1,937).

In the present study, only discrete samples with HPLC determinations are considered for the statistical analysis. They are coupled with the attenuation coefficient determined at the same depth. Because the transmissometer has been

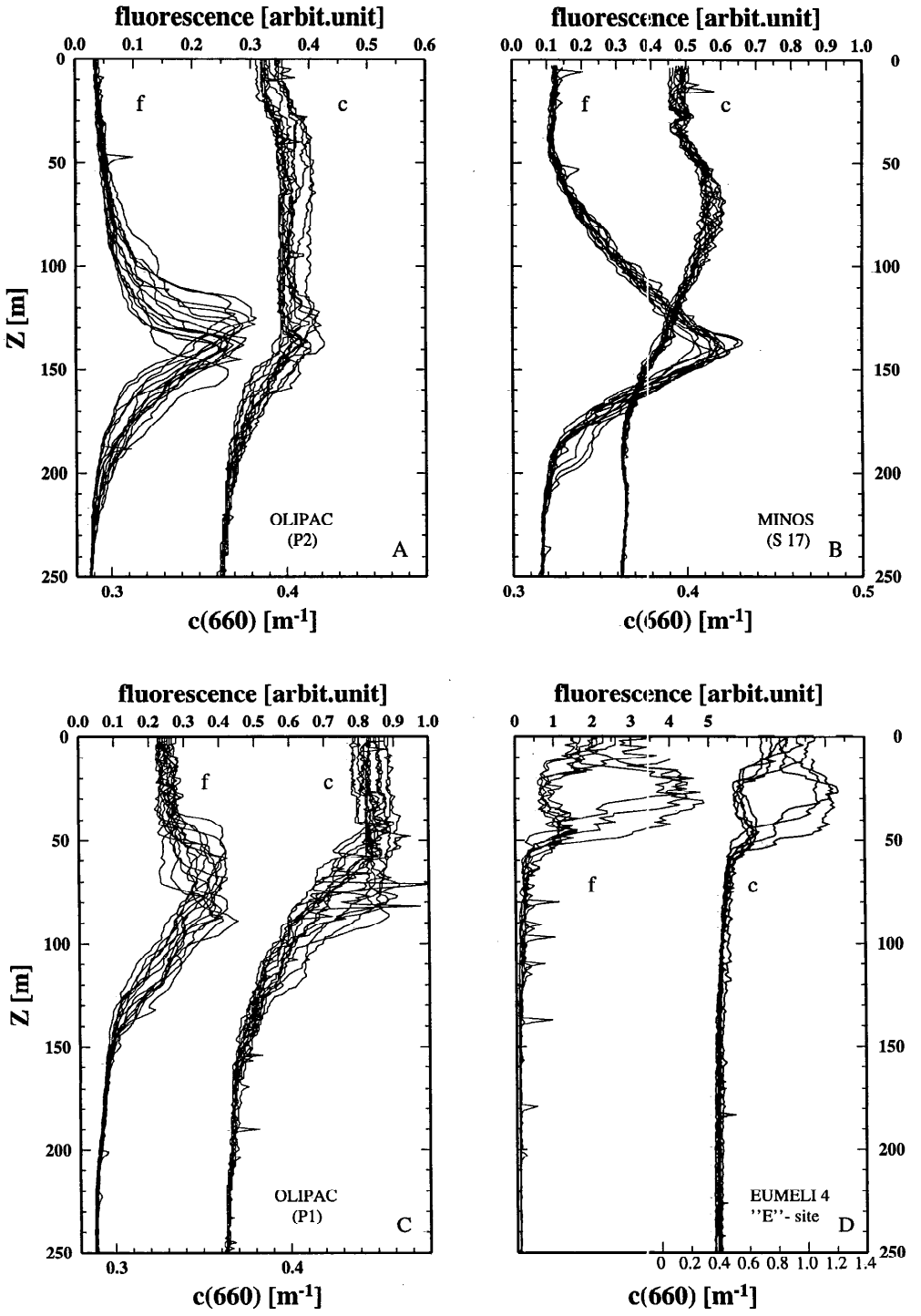

Fig. 2. Selected examples of simultaneous nightly records of beam attenuation and chlorophyll fluorescence (no near-surface photoinhibition effect). For clarity, the scales differ between the panels. Ultra-oligotrophic situations are illustrated by panels A and B, with conspicuous DCM without impact (B) or with minute impact (A) on the attenuation profiles. The algal content in the near-surface layer is higher in P1 than in P2, and the DCM is less prominent, with the result of a quasi-uniform c profile from the surface down to the DCM. In the eutrophic situation (panel D), a tight correlation exists between the two plotted quantities. Temporal variations between the beginning and the end of the night, detectable on the c profiles, are not discussed in the present study.

Table 2. Results of regressions expressed under the form $c_p(660) = \alpha[\text{Chl}]^{\beta}$ for various subsets of data. Subset 1, BOFS and OMEX data (North Atlantic); subset 2, OLIPAC, EqPac, EUMELI 3, EUMELI 4, and MINOS data (tropical Atlantic and Pacific Oceans, Mediterranean Sea); subset 3, BATS and HOTS—time-series stations near Bermuda and Hawaii, respectively. Separate regressions are also provided for four layers, Z_{90} layer, homogeneous layer, deep layer, and all depths (*see text*) (n.s., not significant; *see* Table 1 for definitions of terms).

Subset	Z_{90}-layer				Homogeneous layer				All depths			
	α	β	r^2	N_{sat}	α	β	r^2	N_{hl}	α	β	r^2	N_{all}
1	0.464	0.919	0.80	109	0.382	0.906	0.75	240	0.326	0.876	0.82	484
2	0.278	0.634	0.80	269	0.268	0.632	0.813	455	0.120	0.508	0.36	1,620
3	n.s		0.10	57	0.103	0.358	0.31	155	0.133	0.641	0.46	683
2+3	0.246	0.601	0.71	326	0.252	0.635	0.76	610	0.130	0.601	0.44	2,303
1+2+3 All	0.407	0.795	0.89	435	0.347	0.766	0.88	850	0.189	0.751	0.60	2,787
1+2+3, deep layer*									0.124	0.661	0.54	1,937

* All depths minus the homogeneous layer (i.e. $N_{all} - N_{hl}$).

operated in association with a fluorometer (FL 3000, SeaTech), most of the time, it is possible to convert the vertical profiles of fluorescence by algae into equivalent chlorophyll profiles, and then to compare these profiles with those of attenuation. Such a fluorescence-to-chlorophyll conversion can only be made by interpolating between those depths where the fluorescence signal has been calibrated through the HPLC determination. For the statistical analysis there is objectively no real gain in information when such an expanded and redundant dataset is created; nonetheless, for some figures displayed later, the comparative use of both continuous profiles can offer visual advantages.

After calibration and processing, the transmissometer provides c, the attenuation coefficient for natural water, which must be corrected for the attenuation by pure (particle-free) seawater to derive the particle attenuation coefficient, c_p. With a view to eliminating the uncertainties resulting from imperfect calibrations, the value of c, as observed at the bottom of the column investigated (at 200 or 250 m) where [Chl] is nearly zero, has been considered as being representative of the c value for particle-free water. This value actually is always lower than 0.37 m^{-1} (*see* Fig. 2), and thus is never far from that of pure water (0.358 m^{-1}; Bishop 1986), except at the E site (EUMELI No. 4, Fig. 2D). At site E, c remained slightly higher (0.39 m^{-1} on average), in agreement with a higher particulate organic carbon content at 200–250 m (~0.15 mg C m^{-3} vs. 0.05 at the M and O sites). By subtracting the local deep value, only the excess of attenuation that is related to the presence in the upper layers of chlorophyll-bearing particles and of their retinue is accounted for. The possible effects of dissolved absorbing substance or of local backscattering background (if any) are also greatly reduced by this procedure. Because measurements in OMEX stations were generally restricted to the upper 120 m, the factory-calibrated value (0.364 m^{-1}) was subtracted, which is safe since the calibration of the sensor was carefully checked (Lowry pers. comm.).

After the deep (or the calibrated) value is subtracted, the lower significant value is estimated to be $\sim 2 \times 10^{-3}$ m^{-1}. Interestingly, this value is similar to that which can be computed for the effect of a heterotrophic bacteria background. Such bacterial abundance at ~200 m ranges from 1 to 3 $\times$ 10^{11} cells m^{-3} at the EUMELI sites (Dufour and Torréton 1996), as also recorded in the tropical Pacific (OLIPAC cruise, Vaulot and Marie unpubl. data; Ducklow et al. 1995). By assuming a cell diameter of 0.5 μm and a refractive index of 1.05 (relative to that of water), the scattering coefficient (at 660 nm) of this bacterial population would be between 1 and 3 $\times$ 10^{-3} m^{-1} (Morel and Ahn 1990). Another scattering background could originate from the eolian dust transport and deposition. Near the Mauritanian coast and in the Mediterranean, Saharan dust outbreaks may occasionally occur. This was not the case during the EUMELI and MINOS cruises. Visual observation, as well as aerosol optical thickness measurements, made from the ship or from Sal Island (Cap Verde Islands) demonstrated that no particular dust event happened before or during these cruises (Moulin et al. 1997). Settling mineral particles were not detected in sediment traps, and anomalously high attenuation values in the water column below the photic zone were never observed during the EUMELI or MINOS cruises.

At this point, it is necessary to verify that b_p and c_p are directly comparable, and then to estimate the contribution of absorption to the attenuation coefficient. The absorption coefficient for phytoplankton in natural seawaters with varying chlorophyll concentration has been studied (Bricaud et al. 1995); at 660 nm, this coefficient, a_ϕ, can be expressed as a function of [Chl] according to

$$a_\phi(660) = 0.012[\text{Chl}]^{0.878}. \quad (2)$$

A similar relationship for a_p, the absorption coefficient by the total particulate matter retained on a GFF filter, has also been established (A. Bricaud pers. comm.):

$$a_p(660) = 0.014[\text{Chl}]^{0.817}. \quad (3)$$

Despite a rather low coefficient of determination ($r^2 = 0.27$), this expression allows the effect of absorption to be roughly estimated. For the [Chl] range considered here, extending from 0.02 to 4.5 mg m^{-3}, a_p would vary between 0.00057 and 0.048 m^{-1} according to Eq. 3. These values are negligible (<3%) compared to those of c_p, amounting to ~0.03 and 1.5 m^{-1} for the same extrema in [Chl], as seen in Fig. 3A. Actually, these values are totally insignificant compared to the (natural as well as instrumental) fluctuations that affect the c_p values, as well as to the scatter seen in Fig. 3. There-

fore, in what follows, c_p can be safely considered as equivalent to b_p and discussed as such.

Results and first analysis

All c_p values (N = 2,787) are plotted vs. their associated [Chl] values in Fig. 3A. Specific symbols are used to discriminate the three vertically stratified subsets. The general disposition of the data in this graph resembles that previously found for the b_p–[Chl] relationship (Gordon and Morel 1983). The band (in Gordon and Morel's fig. 5a) delimiting the domain where case 1 waters were confined is reproduced in Fig. 3B after having been slightly shifted down by a factor 0.83; this factor assumes a scattering spectral dependency expressed by λ^{-1}. The upper and lower A values become 0.38 and 0.10, and the average value becomes 0.25, when corrected for the spectral shift from 550 to 660 nm. A $\lambda^{-0.5}$ dependency, with a resulting factor of 0.91, as proposed by Voss (1992), could as well be used without appreciable impact.

From the examination of Fig. 3A (*see* also Table 2), and in reference to the previous findings, several important points emerge. For the whole dataset the general slope (i.e. the exponent) is slightly higher than that appearing in Eq. 1. Indeed, when all depths are pooled together, the regression analysis performed on the log-transformed data leads to

$$c_p(660) = 0.189[\mathrm{Chl}]^{0.751} \quad (\text{with } r^2 = 0.60 \text{ and } N_{all} = 2{,}787), \tag{4}$$

and the coefficient (0.189) falls slightly below the previous A value (0.25, from Eq. 1). For the near-surface layer, limited by the depth Z_{90}, the separate analysis results in

$$c_p(660) = 0.407[\mathrm{Chl}]^{0.795} \quad (\text{with } r^2 = 0.89 \text{ and } N_{sat} = 435), \tag{5}$$

whereas for the homogeneous layer it becomes

$$c_p(660) = 0.347[\mathrm{Chl}]^{0.766} \quad (\text{with } r^2 = 0.88 \text{ and } N_{hl} = 850). \tag{6}$$

These last two equations are not significantly different according to Fisher's combined probability test. They are numerically very close, as Eq. 5 provides c_p values exceeding those from Eq. 6 by 2–20% when [Chl] varies from 0.01 to 4 mg m^{-3}. If the subset corresponding to the homogeneous layer is subtracted from the full dataset, only the deep values are kept (bottom line in Table 2), and the regression analysis for these data leads to

$$c_p(660) = 0.124[\mathrm{Chl}]^{0.661} \quad (\text{with } r^2 = 0.54 \text{ and } N_{dl} = 1{,}937). \tag{7}$$

There is more scatter in this particular subset, in particular in the domain of extremely low chlorophyll concentrations where both [Chl] and c_p are less accurately determined (recall that c_p is known with an accuracy $\leq 2 \times 10^{-3}$ m^{-1}). The low coefficient (0.124) in this equation is not unexpected, for in deep waters the increase in cellular chlorophyll content, and thus a diminishing number of cells per unit of chlorophyll, may account for a relative reduction in scattering. A lesser proportion of other (nonalgal) accompanying particles could also contribute to this reduction.

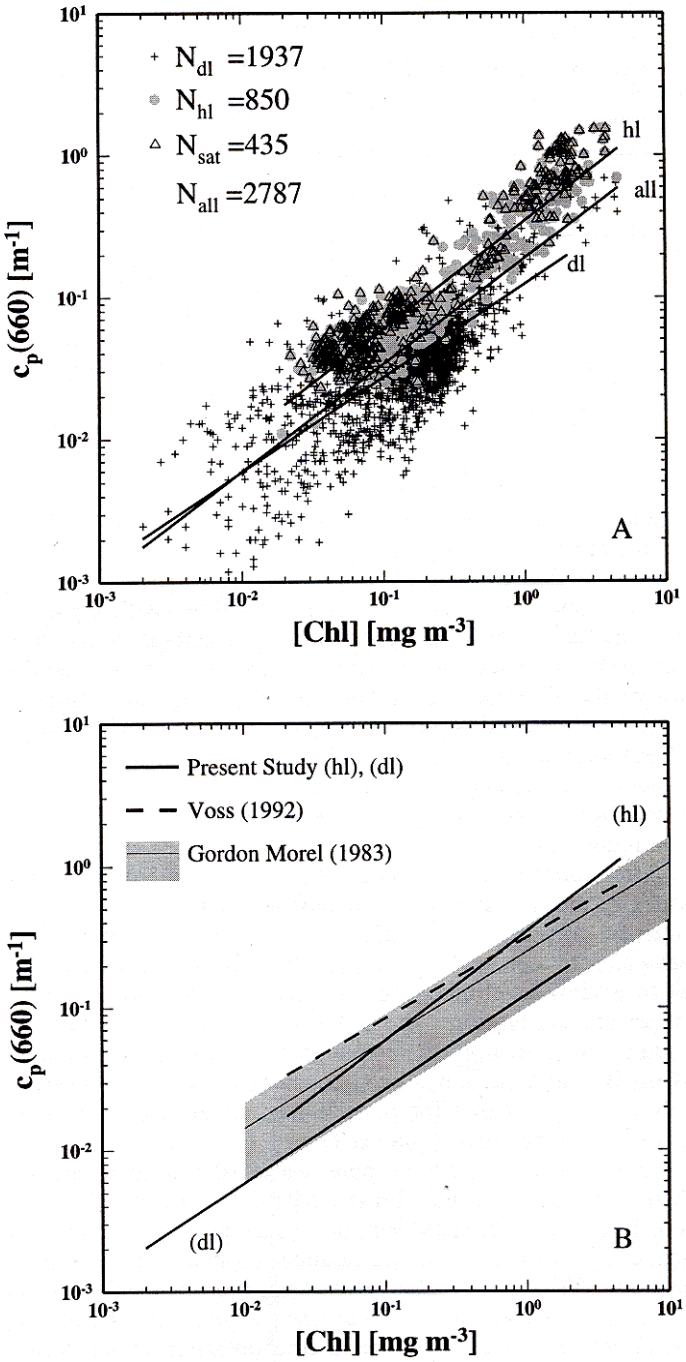

Fig. 3. Plot of all [Chl]–c_p couples according to logarithmic scales; the regression lines for all data pooled together (Eq. 4) and for the data belonging to the homogeneous layer (Eq. 6) or the deep layer (Eq. 7) are also shown in panel A; these various subsets (*see* text and Table 2) are identified by specific symbols. In panel B, regression lines are shown that correspond to Eq. 6 and 7 as well as to Voss' regression line. These lines are superimposed on the shaded band for case 1 waters, as defined by Gordon and Morel (1983).

Compared to the value of 0.62 in Eq. 1, the increase in the exponents appearing in Eq. 4, 5, and 6 essentially originates from the inclusion of the North Atlantic data (not represented in the Gordon–Morel previous analysis); in this

zone, most of the [Chl] values are >1 mg m^{-3}, and c_p values are >0.5 m^{-1}. Regression analyses restricted to the BOFS and OMEX data (subset 1 in Table 2) produce, regardless of the layer considered, exponents distinctly larger than those obtained for the other oceanic areas (subsets 2 and 3, which show exponents close to 0.62). The same statement holds true for the coefficients, notably higher for subset 1 than for other oceanic areas (subsets 2 and 3). Even outside of specific coccolithophore blooms (Ackleson et al. 1994), it is known that coccolithophorids and detached liths are episodically abundant in the North Atlantic (*see* e.g. Holligan et al. 1983; Jickells et al. 1996), and likely are at the origin of changes in optical coefficients as are those detected through separate regression analysis. The presence of such particulate calcite debris increases the scattering coefficient (Bricaud and Morel 1986; Balch et al. 1989), and even can create "anomalous" case 1 waters (Gordon et al. 1988), with extremely high scatterance and reflectance.

Subset 2 includes [Chl] values >1 mg m^{-3}, which were observed at the eutrophic EUMELI site and occasionally at the mesotrophic site (both at ~20°N; *see* map in Fig. 1). In these locations, the algal populations were dominated by diatoms (E site) or by cyanobacteria (M site) (Morel 1997). The c_p values determined in these relatively Chl-rich waters, but in low latitudes, remain below those found farther to the north. Accordingly, the coefficients and exponents for subset 2 are lower than those for subset 1, in particular when the Z_{90} layer is considered (*see* values in Table 2). The low value of the exponent found for the BATS and HOTS data, associated with a low coefficient of determination (subset 3 in Table 2), actually results from the clustering of all these data within a restricted range of values, centered on low [Chl] and c_p values where the signal-to-noise ratio is unfavorable (*see* Table 1).

The coefficients in Eq. 5 or 6, on one hand, and in Eq. 7, on the other hand, are compatible with the maximal and minimal values of A in Eq. 1. The agreement between these previous results and those presented here is clearly seen in Fig. 3b. The spreading of the points for all depths in Fig. 3A is definitely high ($r^2 = 0.60$). The band demarcating case 1 waters in Gordon and Morel's figure (reproduced in Fig. 3B) has already acknowledged that c_p cannot be predicted from [Chl] within a factor better than 3 (actually +50%, −60% with respect to the mean). This factor is not at all reduced for the recent dataset. For the near-surface layer or the homogeneous layer, however, the scatter is considerably less and r^2 is increased up to 0.88, so that the predictive ability is somewhat better and would correspond to a factor of ~2 (instead of ~3) when all depths have been confounded. It has been verified that such a lack of tightness does not result from having pooled diverse sources of data, because separate, cruise-by-cruise analyses do not provide improved (local) correlation and reduced scatter.

There was also a lot of scatter around the relationship obtained by Voss (1992), which was

$$c_p(490) = 0.390[\text{Chl}]^{0.57}. \quad (8a)$$

By using his spectral relationship, this equation can be rewritten for the 660-nm wavelength as

$$c_p(660) = 0.314[\text{Chl}]^{0.57}, \quad (8b)$$

which is also shown for comparison in Fig. 3B. The relationship of Voss consistently agrees with those found here for the homogeneous or near-surface layers, as well as with the upper limit indicated by Gordon and Morel, who stated (as a comment to their Fig. 5a) that "Surface waters are, in most cases, represented by points close to the upper limit."

Another approach can be used to understand the link between c_p (or b_p) and the suspended particle content. Instead of [Chl], the particulate organic concentration, POC, can be adopted as being likely a better descriptor of the total (animate and inanimate) particle content for upper layers in case 1 waters. An almost linear relationship between b_p and POC was already suggested (Morel 1988) by the likeness of the exponents appearing in Eq. 1 and in another empirical relationship, which was established between POC and [Chl] and expressed as (eq. 25 in Morel 1988)

$$\text{POC} = 90[\text{Chl}]^{0.57}, \quad (9)$$

where POC is expressed in mg C m^{-3}. Compared with Eq. 8b above, this expression suggests a perfect linear relationship between c_p and POC, and combined with Eq. 1, it provides the following quasilinear relationship:

$$b_p(550) = B[\text{POC}]^{1.088}, \quad (10)$$

where B is either 0.0090 or 0.0034 (in correspondence with the two extreme A values in Eq. 1). The two straight lines using these values (becoming 0.0075 and 0.0028 at 660 nm) are shown in Fig. 4 and compared to the data. Indeed, considerable ($N = 642$) paired data for both POC and c_p were collected during the BOFS and HOTS experiments. The data relevant to the upper homogeneous layer, as previously identified, are shown with distinct symbols. A regression for this subset ($N = 297$ data) leads to a significant ($r^2 = 0.92$), almost linear relationship (also displayed in Fig. 4):

$$c_p(660) = 0.0010[\text{POC}]^{1.17}. \quad (11)$$

The compatibility between the previous expression (Eq. 10) and present data (leading to Eq. 11) is well ensured. The linear correlation established by Gardner et al. (1993) during a spring bloom in the North Atlantic, which was expressed as

$$c_p(660) = 0.00264[\text{POC}], \quad (12)$$

is also numerically equivalent within the scatter affecting the data.

Discussion and conclusions

The nonlinear character of the dependence of b_p (or c_p) on [Chl] within the whole chlorophyll concentration range and the noise in the correlation between these two quantities observed for surface waters are the main results that warrant further discussion. Both of these aspects are not disjoined. Linearity can only be expected if two obvious conditions are fulfilled. First, the relative size distribution and the particle chemical composition (which governs the refractive index) must remain unchanged; only the bulk seston concentration may vary, as if the same particle assemblage were more or less diluted. In such a case, c_p will be linearly correlated

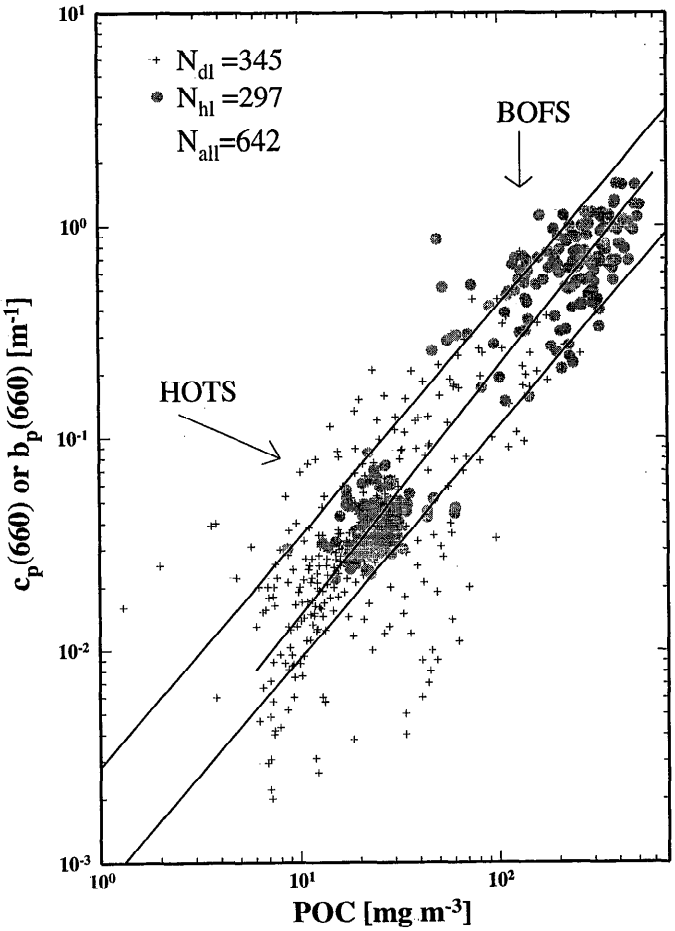

Fig. 4. Log–log plot of all the particulate organic carbon data (POC) and associated c_p values, determined during the BOFS and HOTS experiments as indicated (note that they are not in the same range). The regression line computed (Eq. 11) for the homogeneous layer data only and the two lines corresponding to Eq. 10 (with its two coefficients, *see text*) are superimposed on the data. The correlation etablished by Gardner et al. (1993) (Eq. 12) is very close to the upper line.

with the volume or mass concentration. The slope in this linear relationship depends on the characteristics (size distribution, refractive index, and to a lesser extent shape) of the seston assemblage (*see* e.g. Baker and Lavelle 1984; Spinrad 1986). This slope changes from place to place, even if only deep waters are considered (Bishop 1986). Second, assuming that the first condition is satisfied, the linearity can be preserved in the relationships between c_p and POC or [Chl] only if the POC-to-seston or the Chl-to-seston ratios (wt/wt) are constant.

Concerning the first condition, it is worth recalling what is the size range involved in the formation of the scattering coefficient in oceanic waters. By assuming particle size distributions of the Junge type, with exponents not far from −4 and a mean relative index of refraction close to 1.05, it follows that those particles having sizes between ~0.5 and 10 μm are the main contributors (>95%) to the formation of b_p (*see* fig. III-8 in Morel [1973], where the Junge exponent and the refractive index were varied within reasonable limits; *see* also Morel and Ahn 1991; Stramski and Kiefer 1991). To the extent that the particle-phase function remains rather steady in shape for various oceanic waters (Petzold 1972; Morel 1973; Mobley 1994), the size distribution and the refractive index cannot experience too large variations with respect to figures given above, so that the size range mentioned above is, at least roughly, valid in most circumstances. There is enough variability in particle optical characteristics, however, to impede the prediction of any ubiquitous relationship between b_p and the particle load.

Concerning the second condition, and when using [Chl] as an index for constructing bio-optical models, the situation becomes even more complicated. In effect, the Chl-to-seston ratio is known to vary widely in oceanic waters. The proportions between algal and nonalgal compartments may change and actually do in a more or less regular manner; that is, when the chlorophyll content increases a relative decrease of the nonalgal material influence seems to be the rule (Gordon and Morel 1983; Gordon et al. 1988; Morel 1988). In addition, inside the sole algal compartment, the chlorophyll content per cell also varies widely. In effect, interspecific variability in cellular chlorophyll concentration is large, and intraspecific variation also occurs, in particular as a result of photoacclimation (*see* e.g. Falkowski 1980). Therefore, linear relationships between c_p and [Chl] are not to be expected except in particular conditions. Even in a given location, as soon as all depths are considered, the linearity could be the rule only if the (algal and nonalgal) population remains qualitatively homogeneous vertically, which is not the most common situation (Kitchen and Zaneveld 1990), but may exist when vigorous vertical mixing occurs. Contrasted examples are provided in Fig. 5 by displaying c_p–[Chl] diagrams that are typical of various trophic conditions and hydrologic structures.

In mesotrophic and eutrophic environments with mixed layers thicker than the euphotic layer, as found during the EUMELI cruise No. 4 (Morel 1996), the well-mixed populations satisfy the conditions for linearity. This is reflected by c_p–[Chl] diagrams with a one-to-one slope and concomitant decrease in both quantities along with depth (Fig. 5F). The chlorophyll-specific particulate attenuation coefficient, c_p*, defined as the ratio of c_p to [Chl] (Mitchell and Kiefer 1988), is roughly constant in these examples and amounts to ~0.4 or 0.5 m^2 (mg Chl)$^{-1}$. The algal populations in these two environments, however, differ; that is, they are diatom-dominated in the E site and cyanobacteria-dominated in the M site. In the North Atlantic BOFS stations (not shown in Fig. 5), 1 : 1 slopes are also derived for the upper layers, as can be anticipated from the high coefficient and exponent close to one (first line in Table 2). The c_p* values are similar to those in E and M sites (~0.5 m^2 (mg Chl)$^{-1}$). Within deeply mixed waters in the Drake Passage, with [Chl] typically between 0.5 and 0.8 mg m^{-3}, Mitchell and Holm-Hansen (1991) reported c_p* values of ~0.35 m^2 (mg Chl)$^{-1}$ in December–January. In February–March at the same location (also at another location within an active bloom), c_p* values were in the 0.1–0.2 m^2 (mg Chl)$^{-1}$ range. This decrease was attributed (Mitchell and Holm-Hansen 1991) to a chronic low-light adaptation of the algal population, with the con-

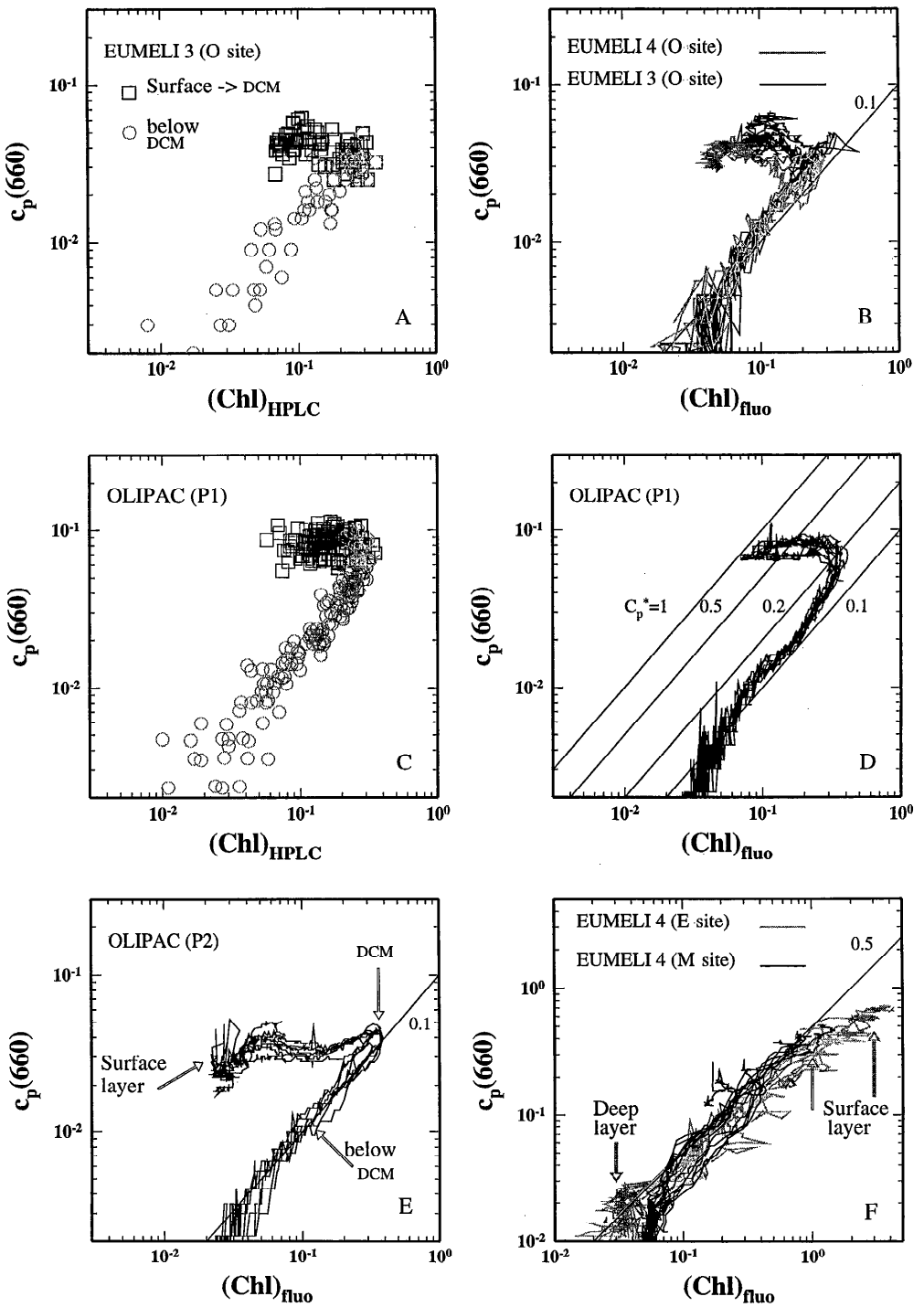

Fig. 5. For selected stations, diagrams showing how the quantities c_p and [Chl] vary with depth. They are constructed either with the [Chl] values determined at discrete depths via HPLC (panels A and C) or (other panels) with the [Chl] profiles derived from the fluorescence profiles after HPLC calibration (only nightly profiles are used). These plots are similar to those in Kitchen and Zaneveld (1990), apart from the replacement of fluorescence by chlorophyll values. Note the change in scales for the eutrophic and mesotrophic stations (EUMELI 4). The straight lines drawn with a 1 : 1 slope correspond to discrete values of the chlorophyll-specific particle attenuation coefficient, c_p^*, expressed in m^2 (mg Chl)$^{-1}$ and with values as indicated.

sequence of a significant increase in chlorophyll per cell. Also in Antarctic waters (in the Belligshausen Sea), Sagan et al. (1995) found c_p* values from 0.1 to 0.4 m^2 (mg Chl)$^{-1}$ inside an extensive phytoplankton bloom, whereas outside this area, values were between 0.4 and 0.9 m^2 (mg Chl)$^{-1}$. In the western Mediterranean Sea during a vernal bloom, b_p* (c_p*) values of 0.22 m^2 (mg Chl)$^{-1}$ were observed in the upper layer (fig. 5B in Gordon and Morel 1983).

Situations from ultra-oligotrophic (Fig. 5A–D) to moderately oligotrophic (Fig. 5E) have in common a peculiarly shaped diagram (called Λ-shape in Kitchen and Zaneveld 1990). Between the surface and the DCM, a more or less extended horizontal segment develops. It begins with a cluster of data corresponding to the upper part of the mixed layer, where the c_p* values are ~1 m^2 (mg Chl)$^{-1}$. Interestingly, similar values are found in the tropical Pacific and Atlantic Oceans, as well as in the Mediterranean Sea (MINOS cruise, not shown). Below this layer, [Chl] increases while c_p (and the number of scattering particles) remains steady, so that c_p* progressively diminishes. The extremum in these diagrams always coincides with the DCM, and the associated c_p* values are close to 0.2 m^2 (mg Chl)$^{-1}$. Below the chlorophyll maximum and toward the deeper aphotic levels another linear segment takes place that follows a 1 : 1 slope. Such a linearity reflects a "mixing rule," i.e. a downward progressive dilution of approximately the same particle assemblage (algal cells, heterotrophic bacteria, and detritus). At these depths, below the euphotic depth, the photoacclimation is almost reached, and thus the chlorophyll contents per cell vary only slightly. The c_p* values corresponding to these linear segments are steadily close to 0.1 m^2 (mg Chl)$^{-1}$ (slightly less in Mediterranean), in spite of a progressive replacement of prochlorophytes by pico-eukaryotes as predominant species (*see* e.g. Partensky et al. 1996; Claustre and Marty 1995). This general c_p* vertical pattern (typical of oligotrophic waters), as well as the high values near the surface, are perfectly put in evidence in the meridional section in the equatorial Pacific (140°W) presented by Sung Pyo Chung et al. (1996).

From the relationship that is valid on average for the near-surface layer (Eq. 5), c_p* can be straightforwardly derived as a function of [Chl]:

$$c_p^*(660) = 0.407[\text{Chl}]^{-0.20}. \quad (13)$$

Note that the c_p* value is sometimes suggested as an index for discriminating case 1 and case 2 waters, and that the criterion $c_p^* > 0.5$ m^2 (mg Chl)$^{-1}$, used for identifying case 2 waters (Sagan et al. 1995), does not seem appropriate. Indeed, according to Eq. 13 this threshold is surpassed in most oceanic case 1 waters as soon as [Chl] is <0.40 mg m^{-3}; for oligotrophic waters in near-surface layer, for instance, c_p* is generally ~1 m^2 (mg Chl)$^{-1}$. If turbid case 2 sediment-loaded waters consistently exhibit high c_p* values, the discriminating threshold value must be specified. Similar to what was proposed in Gordon and Morel (1983), consideration of Eq. 5 and Fig. 3A can help to establish a criterion. The data in this figure (which indubitably belong to case 1 waters) remain below a line, which, for numerical convenience, is forced to include the same exponent as in the near-surface waters expression (Eq. 5):

$$c_p(660) = 0.65[\text{Chl}]^{0.80}. \quad (14)$$

When transferred to the wavelength 550 nm, the above coefficient becomes 0.78, which is considerably larger than that previously proposed (0.45 in Gordon and Morel 1983) for $b_p(550)$, or was adopted in the processing of ocean color satellite imagery (0.5 in Bricaud and Morel 1987).

Attempts to explain the local c_p* values, or the relationship between vertical c_p and [Chl] profiles, have already been made (Sung Pyo Chung et al. 1996; Durand and Olson 1996). Such attempts rest on the knowledge of the scattering cross sections of the identified microbial organisms, and with this aim, databases of the single-particle optical properties of marine microbial particles are progressively built up (Stramski and Mobley 1997; Mobley and Stramski 1997). Such an analytical approach (*see* also attempts in Morel and Ahn 1991) or such case-by-case studies are out of the scope of the present work, which solely attempts to derive empirical relationships for general use in various trophic regimes.

In conclusion, the present analysis of recent data, obtained in methodological conditions better than those used in the past, strengthens the previously observed trends and allows some refinements to be introduced in optical modeling of case 1 waters. First, the nonlinear character of the relationship between scattering (or attenuation at 660 nm) and chlorophyll concentration is confirmed. Locally, or for a certain depth interval and peculiar particles assemblages, linear relationships may exist. Nevertheless, when they are pooled together to encompass the entire chlorophyll range, such a merging results in a global nonlinear effect, reflected by exponents on the order of 0.7 that apply to [Chl]. This nonlinear biological effect essentially originates from the continuous and nonlinear change in the Chl-to-POC ratio, as, *a contrario,* testified by the existence of a quasilinear relationship between scattering (or attenuation) and POC.

Second, the very upper layer, involved in remote-sensing applications, or the homogeneous part of the mixed layer exhibits specific bio-optical properties, and thus produces relationships (Eq. 5 and 6) differing from that describing the deep layer (Eq. 7). The adoption, as done before, of a unique expression when modeling case 1 waters is certainly to be discouraged, in particular if scattering vertical structures are to be reconstructed from the vertical chlorophyll profiles. This point was rightly stressed by Kitchen and Zaneveld (1990), particularly for backscattering, but holds true also for scattering. For remote-sensing applications, the adoption of Eq. 5 is definitely thought to be a better choice over Eq. 1. This proposed expression leads to c_p (b_p) values that are similar to those provided by Eq. 1 when systematically operated with its upper value. Eq. 5 appears more robust to the extent that c_p can be predicted from [Chl] within a factor of 2 (instead of 3 with Eq. 1).

Finally, contrary to expectation, a less noisy relationship was not derived from the present data, despite methodological improvements in their determination. The natural variability at local and then at global scales prevents obtaining tighter relationships between optical properties and [Chl]. In this respect, it must be added that arctic and antarctic waters, with presumably low-light-adapted phytoplanktonic populations, could depart from the general trend and thus be in-

adequately described by the present expressions. Future improvements, including a regionalization of the predictive algorithms, still require additional measurements in various oceanic conditions.

References

ACKLESON, S. G., W. M. BALCH, AND P. M. HOLLIGAN. 1994. Response of water-leaving radiance to particulate calcite and chlorophyll a concentrations: A model for Gulf of Maine coccolithophore blooms. J. Geophys. Res. **99:** 7483–7499.

BAKER, E. T., AND J. W. LAVELLE. 1984. The effect of particle size on the light attenuation coefficient of natural suspensions. J. Geophys. Res. **89:** 8197–8203.

BALCH, W. M., R. W. EPPLEY, M. R. ABBOTT, AND F. M. H. REID. 1989. Bias in satellite-derived pigment measurements due to coccolithophores and dinoflagellates. J. Plankton Res. **11:** 575–581.

BARTZ, R., J. R. V. ZANEVELD, AND H. PARK. 1978. A transmissometer for profiling and moored observations in water. Proceeding of the Society of Photo-Optical Instrumentation Engineering. Ocean Optics **160:** 102–108.

BISHOP, J. K. B. 1986. The correction and suspended particulate matter calibration of SeaTech transmissometer data. Deep-Sea Res. **33:** 121–134.

BRICAUD, A., M. BABIN, A. MOREL, AND H. CLAUSTRE. 1995. Variability in the chlorophyll-specific absorption coefficients of natural phytoplankton: Analysis and parameterization. J. Geophys. Res. **100:** 13,221–13,332.

———, AND A. MOREL. 1986. Light attenuation and scattering by phytoplanktonic cells: A theoretical model. Appl. Optics **25:** 121–134.

———, AND ———. 1987. Atmospheric correction and interpretation of marine radiances in CZCS imagery: Use of a reflectance model. Oceanol. Acta Spec. Publ: 33–50.

CLAUSTRE, H., AND J. C. MARTY. 1995. Specific phytoplankton biomasses and their relation to primary production in the tropical north Atlantic. Deep-Sea Res. **42:** 1475–1493.

CULLEN, J. J. 1982. The deep chlorophyll maximum: Comparing vertical profiles of chlorophyll *a*. Can. J. Fish. Aquat. Sci. **39:** 791–803.

DUCKLOW, H. W., H. L. QUINBY, AND A. CARLSON. 1995. Bacterioplankton dynamics in the equatorial Pacific during the 1992 El Niño. Deep-Sea Res. II **42:** 621–638.

DUFOUR, P., AND J.-P. TORRÉTON. 1996. Bottom-up and top-down control of bacterioplankton from eutrophic to oligotrophic sites in the tropical northeastern Atlantic ocean. Deep-Sea Res. **43:** 1305–1320.

DURAND, M. D., AND R. J. OLSON. 1996. Contributions of phytoplankton light scattering and cell concentration changes to diel variations in beam attenuation in the equatorial Pacific from flow cytometric measurements of pico-, ultra- and nanoplankton. Deep-Sea Res. II **43:** 891–906.

FALKOWSKI, P. G. 1980. Light-shade adaptation in marine phytoplankton, p. 99–119. *In* Primary productivity in the sea. Environmental science research. V. 19. Plenum.

GARDNER, W. D., I. D. WALSH, AND M. J. RICHARDSON. 1993. Biophysical forcing of particle production and distribution during a spring bloom in the north Atlantic. Deep-Sea Res. **40:** 171–195.

GIBBS, R. J. 1979. Chlorophyll *b* interference in the fluorometric determination of chlorophyll *a* and phaeo-pigments. Aust. J. Mar. Freshw. Res. **30:** 597–606.

GORDON, H. R., O. B. BROWN, R. H. EWANS, AND OTHERS. 1988. A semianalytical radiance model of ocean color. J. Geophys. Res. **93**(D9): 10,909–10,924.

———, AND W. R. MCCLUNEY. 1975. Estimation of the depth of sunlight penetration in the sea for remote sensing. Appl. Optics **14:** 413–416.

———, AND A. MOREL. 1983. Remote assessment of ocean color for sattelite visible imagery. A review, p. 1–114. *In* R. T. Barber, C. N. K. Mooers, M. J. Bowman, and B. Zeizschel [eds.], Lecture notes on coastal and estuarine studies. Springer-Verlag.

HOLLIGAN, P. M., M. VIOLLIER, D. S. HARBOUR, P. CAMUS, AND M. CHAMPAGNE-PHILIPPE. 1983. Satellite and ship studies of coccolithophore production along a continental shelf edge. Nature **304:** 339–342.

HOLM-HANSEN, O., C. J. LORENZEN, R. W. HOLMES, AND J. D. STRICKLAND. 1965. Fluorometric determination of chlorophyll. J. Cons. Int. Explor. Mer. **30:** 3–15.

JEFFREY, S. W., AND G. G. HUMPHREY. 1975. New spectrophotometric equations for determining chlorophylls *a, b,* c_1 and c_2 in higher plants, algae and natural phytoplankton. Biochem. Physiol. Pflanz. **167:** 191–194.

JICKELLS, T. D., P. P. NEWTON, P. KING, R. S. LAMPITT, AND C. BOUTLE. 1996. A comparison of sediment trap records of particle fluxes from 19 to 18°N in the northeast Atlantic and their relation to surface water productivity. Deep-Sea Res. I **43:** 971–986.

KARL, D. M., AND A. F. MICHAELS. 1996. The Hawaiian ocean time-series (HOT) and Bermuda Atlantic time-series study (BATS). Deep-Sea Res. II **43:** 127–128.

KIEFER, D. A., R. J. OLSON, AND O. HOLM-HANSEN. 1976. Another look at the nitrite and chlorophyll maxima in the central north Pacific. Deep-Sea Res. **23:** 1199–1208.

KITCHEN, J. C., AND J. R. V. ZANEVELD. 1990. On the noncorrelation of the vertical structure of light scattering and chlorophyll *a* in case I waters. J. Geophys. Res. **95:** 20,237–20,246.

LOWRY, R. K., P. MACHIN, AND R. N. CRAMER. 1994. BOFS North Atlantic data set. British oceanographic data center CD-ROM. *In* Natural Environment Research Council (eds.).

MITCHELL, B. G., AND O. HOLM-HANSEN. 1991. Bio-optical properties of Antartic Peninsula waters: Differentiation from temperate ocean models. Deep-Sea Res. **38:** 1009–1028.

———, AND D. A. KIEFER. 1988. Variability in pigment specific particulate fluorescence and absorption spectra in the north eastern Pacific ocean. Deep-Sea Res. **35:** 665–689.

MOBLEY, C. D. 1994. Light and water. Radiative transfer in natural waters. Academic.

———, AND D. STRAMSKI. 1997. Effects of microbial particles on ocanic optics: Methodology for radiative transfer modeling and example simulations. Limnol. Oceanogr. **42:** 550–560.

MOREL, A. 1973. Diffusion de la lumière par les eaux de mer; Résultats expérimentaux et approche théorique. Optics of the sea, AGARD lecture series, 63, sect. **3:** 1–76.

———. 1980. In-water and remote measurements of ocean color. Boundary-Layer Meteorol. **18:** 177–201.

———. 1987. Chlorophyll-specific scattering coefficient of phytoplankton. A simplified theoretical approach. Deep-Sea Res. **34:** 1093–1105.

———. 1988. Optical modeling of the upper ocean in relation to its biogenous matter content (case I waters). J. Geophys. Res. **93:** 10,749–10,768.

———. 1996. An ocean flux study in eutrophic, mesotophic and oligotrophic situations: The EUMELI program. Deep-Sea Res. **43:** 1185–1190.

———. 1997. Consequences of a *Synechococcus* bloom upon the optical properties of oceanic case 1 waters. Limnol. Oceanogr. **42:** 1746–1754.

———, AND Y. H. AHN. 1990. Optical efficiency factors of free

living marine bacteria: Influence of bacterioplankton upon the optical properties and particulate organic carbon in oceanic waters. J. Mar. Res. **48:** 145–175.

———, AND ———. 1991. Optics of heterotrophic nanoflagellates and ciliates: A tentative assessment of their scattering role in ocenic waters compared to those of bacterial and algal cells. J. Mar. Res. **49:** 171–202.

———, AND J. F. BERTHON. 1989. Surface pigments, algal biomass profiles, and potential production of the euphotic layer: relationships reinvestigated in view of remote-sensing applications. Limnol. Oceanogr. **34:** 1541–1564.

———, AND L. PRIEUR. 1977. Analysis of variations in ocean color. Limnol. Oceanogr. **22:** 709–722.

MOULIN, C., AND OTHERS. 1997. Long-term daily monitoring of Saharan dust load over ocean using Meteosat ISCCP-B2 data. 2. Accuracy of the method and validation using sun photometer measurements. J. Geophys. Res. **102:** 16,959–16,969.

MURRAY, J. W., E. JOHNSON, AND C. GARSIDE. 1995. A U.S. JGOFS process study in the equatorial Pacific (EqPac): Introduction. Deep-Sea Res. II **42:** 275–293.

PAK, H., D. A. KIEFER, AND J. C. KITCHEN. 1988. Meridional variations in the concentration of chlorophyll and microparticles in the North Pacific ocean. Deep-Sea Res. **35:** 1151–1171.

PARTENSKY, F, J. BLANCHOT, F; LANTOINE, J. NEVEUX, AND D. MARIE. 1996. Vertical structure of picophytoplankton at different trophic sites of the tropical northeastern Atlantic ocean. Deep-Sea Res. **43:** 1191–1213.

PETZOLD, J. T. 1972. Volume scattering functions for selected ocean waters. Scipps Inst. Oceanogr. Publ. **72–78.** 79 p.

SAGAN, S., A. WEEKS, I. ROBINSON, G. MOORE, AND J. AIKEN. 1995. The relationship between beam attenuation and chlorophyll concentration and reflectance in Antartic waters. Deep-Sea Res. II **42:** 983–996.

SMITH, R. C., AND K. S. BAKER. 1978. The bio-optical state of ocean waters and remote sensing. Limnol. Oceanogr. **23:** 247–259.

SPINRAD, R. W. 1986. A calibration diagram of specific beam attenuation. J. Geophys. Res. **91**(C6)**:** 7761.

STRAMSKI, D., AND D. A. KIEFER. 1991. Light scattering by microorganisms in open ocean. Prog. Oceanogr. **28:** 343–383.

———, AND C. D. MOBLEY. 1997. Effects of microbial particles on oceanic optics: A database of single-particle optical properties. Limnol. Oceanogr. **42:** 538–549.

SUNG PYO CHUNG, W. D. GARDNER, M. J. RICHARDSON, I. D. WALSH, AND M. R. LANDRY. 1996. Beam attenuation and micro-organisms: Spatial and temporal variations in small particles along 140°W during the 1992 JGOFS EqPac transects. Deep-Sea Res. II **43:** 1205–1226.

VOSS, K. J. 1992. A spectral model of the beam attenuation coefficient in the ocean and coastal areas. Limnol. Oceanogr. **37:** 501–509.

Received: 3 July 1997
Accepted: 17 November 1997